

---

# Mitigating Label Noise through Data Ambiguation

---

**Julian Lienen**

Department of Computer Science  
Paderborn University  
Paderborn 33098, Germany  
julian.lienen@upb.de

**Eyke Hüllermeier**

Institute of Informatics, LMU Munich  
Munich Center for Machine Learning  
Munich 80538, Germany  
eyke@lmu.de

## Abstract

Label noise poses an important challenge in machine learning, especially in deep learning, in which large models with high expressive power dominate the field. Models of that kind are prone to memorizing incorrect labels, thereby harming generalization performance. Many methods have been proposed to address this problem, including robust loss functions and more complex label correction approaches. Robust loss functions are appealing due to their simplicity, but typically lack flexibility, while label correction usually adds substantial complexity to the training setup. In this paper, we suggest to address the shortcomings of both methodologies by “ambiguating” the target information, adding additional, complementary candidate labels in case the learner is not sufficiently convinced of the observed training label. More precisely, we leverage the framework of so-called superset learning to construct set-valued targets based on a confidence threshold, which deliver imprecise yet more reliable beliefs about the ground-truth, effectively helping the learner to suppress the memorization effect. In an extensive empirical evaluation, our method demonstrates favorable learning behavior on synthetic and real-world noise, confirming the effectiveness in detecting and correcting erroneous training labels.

## 1 Introduction

Label noise refers to the presence of incorrect or unreliable annotations in the training data, which can negatively impact the generalization performance of learning methods. Dealing with label noise constitutes a major challenge for the application of machine learning methods to real-world applications, which often exhibit noisy annotations in the form of erroneous labels or distorted sensor values. This is no less a concern for large models in the regime of deep learning as well, which have become increasingly popular due to their high expressive power, and are not immune to the harming nature of label noise. Existing methods addressing this issue include off-the-shelf robust loss functions, e.g., as in [Wang et al., 2019], and label correction, for example by means of replacing labels assumed to be corrupted [Wu et al., 2021]. While the former appeals with its effortless integration into classical supervised learning setups, methods of the latter kind allow for a more effective suppression of noise by remodeling the labels. However, this comes at the cost of an increased model complexity, typically reducing the efficiency of the training [Liu et al., 2020].

The training dynamics of models in the considered regime have been thoroughly studied [Chang et al., 2017, Arazo et al., 2019, Liu et al., 2020], which in fact entail two learning phases that can be distinguished: Initially, as shown in the left plot of Fig. 1, the model shows reasonable learning behavior by establishing correct relations between features and targets, classifying even mislabeled instances mostly correctly. In this phase, the loss minimization is dominated by the clean fraction, such that the mislabeling does not affect the learning too much. However, after the clean labels are

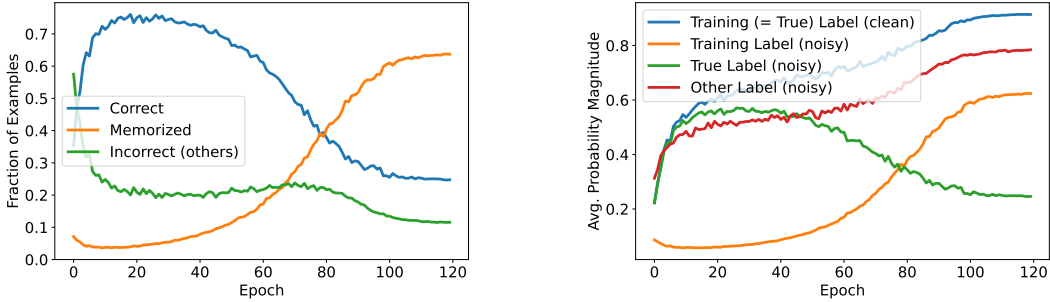


Figure 1: For ResNet34 models trained with cross-entropy on CIFAR-10 with 25 % of corrupted instances (averaged over five seeds), the left plot shows the fractions of examples that are correctly classified, memorized with respect to their corrupted training label, or incorrectly classified with a label other than the ground-truth or training label, confirming the result in [Liu et al., 2020]. The right plot illustrates the predicted probability magnitudes for clean or noisy labels.

sufficiently well fit, the loss minimization starts to concentrate predominantly on the mislabeled part, thereby overfitting mislabels and thus harming generalization.

A closer look at the probabilistic predictions in the first learning phase reveals that the confidence degrees allow for distinguishing between erroneous training labels and the underlying ground-truth classes. The right plot in Fig. 1 illustrates that models are typically not incentivized to optimize for predicting the corrupted training labels in the first epochs, but infer relatively high probability scores for the (unknown) ground-truth class. The learned knowledge of the model at this point could be regarded as a distillation process from the noisy labels – the model is implicitly able to distinguish between clean and noisy instances, and retains only useful information. Evidently, the model *itself* could serve as a source for modeling the beliefs about the ground-truth, taking all (mostly clean) instance-label relations into account to reason about the true labeling. This idea has been adopted by label correction methods that predict *pseudo-labels* for instances that appear to be mislabeled, thus suggesting labels that are considered by the model to be more plausible [Reed et al., 2015, Wu et al., 2021]. Nevertheless, especially in early phases of the training, substituting the original label as a possibly correct information entails the risk of drawing conclusions too hastily, potentially aggravating the negative effects of label noise. Instead, it seems advisable to not completely exclude the possibility of the original training label being the target either to realize a cautious learning behavior, as the learner is still in its infancy and should not discard true labels too early.

Following this motivation, we propose a *complementary* target modeling approach that is guided by the learner’s confidence. Specifically, our approach accounts for the potential existence of other plausible labels beyond the observed training label, which may appear plausible in the context of the overall optimization, while not degrading the initial label’s plausibility either. To achieve this, we employ so-called *supersets* [Liu and Dietterich, 2014, Hüllermeier and Cheng, 2015] to maintain sets of candidate labels modeling the beliefs about the true outcome. In this course, we deliberately “ambiguate” the targets by adding classes to the superset that exceed a specified confidence threshold. More precisely, we represent the ambiguous target information in the form of so-called *credal sets*, i.e., sets of probability distributions, to train probabilistic classifiers via generalized risk minimization in the spirit of label relaxation [Lienen and Hüllermeier, 2021b]. We realize our approach, which we dub *Robust Data Ambiguation* (RDA), in an easy off-the-shelf loss function that dynamically derives the target sets from the model predictions without the need of any additional parameter – this is implicitly done in the loss calculation, without requiring any change to a conventional learning routine. This way, we combine the simplicity of robust losses with the data modeling capabilities of more complex label correction approaches. We demonstrate the effectiveness of our method on commonly used image classification datasets with both synthetic and real-world noise, confirming the adequacy of our proposed robust loss.

## 2 Related Work

Coping with label noise in machine learning contexts is a broad field with an extensive amount of literature in the recent times. Here, we distinguish four views on this issue, namely, robust loss functions, regularization, sample selection and label correction methods. For a more comprehensive overview, we refer to [Song et al., 2020, Wei et al., 2022b] as recent surveys.

**Robust Losses:** The task of designing robust optimization criteria has a long-standing history in classical statistics, e.g., to alleviate the sensitivity towards outliers. As a prominent member of such methods, the mean absolute error (MAE) steps up to mitigate the shortcomings of the mean squared error. When relating to the context of probabilistic classification, analyses link robustness of loss functions towards label noise to the symmetry of the function [Ghosh et al., 2017], leading to suchlike cross-entropy adaptations [Wang et al., 2019, Ma et al., 2020]. A large strain of research proposes to balance MAE and cross-entropy, e.g., by the negative Box-Cox transformation [Zhang and Sabuncu, 2018] or controlling the order of Taylor series for the categorical cross-entropy [Feng et al., 2020], whereas also alternative loss formulations have been considered [Yu et al., 2020, Wei and Liu, 2021]. Besides, methodologies accompanying classical losses for robustness have been proposed, such as gradient-clipping [Menon et al., 2020] or sub-gradient optimization methods [Ma and Fattah, 2022].

**Regularization:** Regularizing losses for classification has also been considered as a mean to cope with label noise. As one prominent example, label smoothing [Szegedy et al., 2016] has shown similar beneficial properties as loss correction when dealing with label noise [Lukasik et al., 2020]. Advancements also enable applicability in high noise regimes [Wei et al., 2022a]. Among the first works building upon this observation, [Arpit et al., 2017] characterizes two phases in learning from data with label noise. First, the model learns to correctly classify most of the instances (including the ground-truth labels of misclassified training instances), followed by the memorization of mislabels. The works shows that explicit regularization, for instance Dropout Srivastava et al. [2014], is effective in combating memorization, improving generalization. Building upon this insight, [Liu et al., 2020] proposes a penalty term to counteract memorization that stems from the (more correct) early-learning of the model. In addition, sparse regularization enforces the model to predict sharp distributions with sparsity [Zhou et al., 2021b]. Lastly, [Iscen et al., 2022] describes a regularization term based on the consistency of an instance with its neighborhood in feature space.

**Sample Selection:** Designed to prevent the aforementioned memorization of mislabeled instances, a wide variety of methods rely on the so-called small loss selection criterion [Jiang et al., 2018, Gui et al., 2021], which is intended to distinguish clean samples the model recognizes well, from which can be learned in an undistorting manner. This distinctions allows to model a range of models, including a gradual increase of the clean sample set with increasing model confidence [Shen and Sanghavi, 2019, Cheng et al., 2021, Wang et al., 2022], co-training [Han et al., 2018, Yu et al., 2019, Wei et al., 2020] or re-weighting instances [Chen et al., 2021]. Furthermore, it makes the complete plethora of classical semi-supervised learning methods amenable to the task of label noise robustness. Here, the non-small loss examples are considered as unlabeled in the first place [Li et al., 2020, Nishi et al., 2021, Zheltonozhskii et al., 2022]. Often, such methodology is also combined with consistency regularization [Bachman et al., 2014], as prominently used in classical semi-supervised learning [Sohn et al., 2020, Liu et al., 2020, Yao et al., 2021, Liu et al., 2022].

**Label Correction:** Traditionally, correcting label noise has also been considered by learning probabilistic transition matrices [Goldberger and Ben-Reuven, 2017, Patrini et al., 2017, Zhu et al., 2022, Kye et al., 2022], e.g., to re-weight or correct losses. In this regard, it has been considered to learn a model and (re-)model labels based on the model predictions jointly [Tanaka et al., 2018]. Closely related to sample selection as discussed before, [Song et al., 2019] proposes to first select clean samples in a co-teaching method, which then refurbishes noisy samples by correcting their label information. Furthermore, Arazo et al. [2019] suggests to use two-component mixture models for detecting mislabels that are to be corrected, thus serving as a clean sample criterion. Moreover, [Wu et al., 2021, Tu et al., 2023] approaches the problem of label correction by a meta-learning formulation that models a two-stage optimization process of the model and the training labels. In addition, [Liu et al., 2022] describes an approach to learn the individual instances' noise by an additional over-parameterization. Finally, ensembling has also been considered as a source for label correction [Lu and He, 2022].

### 3 Method

The following section outlines the motivation behind our method RDA to model targets in an ambiguous manner, introduces the theoretical foundation, and elaborates on how this approach realizes robustness against label noise.

#### 3.1 Motivation

Deep neural networks models, often overparameterized with significantly more parameters than required to fit training data points at hand, have become the de-facto standard choice for most practically relevant problems in deep learning. Here, we consider probabilistic models of the form  $\hat{p} : \mathcal{X} \rightarrow \mathbb{P}(\mathcal{Y})$  with  $\mathcal{X} \subset \mathbb{R}^d$  and  $\mathcal{Y} = \{y_1, \dots, y_K\}$  being the feature and target space, respectively. We denote the training set of size  $N$  as  $\mathcal{D}_N = \{(\mathbf{x}_i, y_i)\}_{i=1}^N \subset \mathcal{X} \times \mathcal{Y}$ , where each instance  $\mathbf{x}_i \in \mathcal{X}$  is associated with an underlying (true) label  $y_i^*$ . The latter is conceived as being produced by the underlying (stochastic) data-generating process, i.e., as the realization of a random variable  $Y \sim p^*(\cdot | \mathbf{x})$ .<sup>1</sup> However, the actual label  $y_i$  encountered in the training data might be corrupted, which means that  $y_i \neq y_i^*$ . Reasons for corruption can be manifold, including erroneous measurement and annotation by a human labeler.

As real-world data typically comprises noise in the annotation process, e.g., due to human labeling errors, their robustness towards label noise is of paramount importance. Alas, models in the regime of deep learning trained with conventional (probabilistic) losses, such as cross-entropy, lack this robustness. As been thoroughly discussed in the analysis of the training dynamics of such models [Chang et al., 2017, Arazo et al., 2019, Liu et al., 2020], two phases can be distinguished in the training of alike models, namely a “correct concept learning” and a *memorization* [Arpit et al., 2017] or *forgetting* [Toneva et al., 2019] phase (cf. Fig. 1). While the model behaves in a desirable manner in the first phase by assimilating reasonable relations between instances and labels, leading to mostly correct predictions on most training instances, the transition to a more and more memorizing model harms the generalization performance.

Looking closer at the learning dynamics in an idealized setting, one can observe that overparameterized models project instances of the same ground-truth class  $y^*$  to a similar feature embedding, regardless of having observed a correct or corrupted training label in the first training phase. Fig. 2 illustrates the learned feature activations of the penultimate layer of a multi-layer perceptron with a classification head trained on MNIST over the course of the training (see the appendix for further experimental details). In the beginning, the learner predicts a relatively high probability  $\hat{p}(y_i^* | \mathbf{x}_i)$  for noisy instances  $(\mathbf{x}_i, y_i)$  despite the observed corrupted training label  $y_i \neq y_i^*$ , as the loss is dominated by the cross-entropy of the clean instances, which leads to a similar marginalization behavior as in the non-corrupted case. Here, the proximity of mislabeled instances to the decision boundary can be related to the “hardness” of instances to be learned, as also been studied in previous work [Chang et al., 2017]. In later stages, the feature activations of the noisy instances shift in a rotating manner, successively being pushed

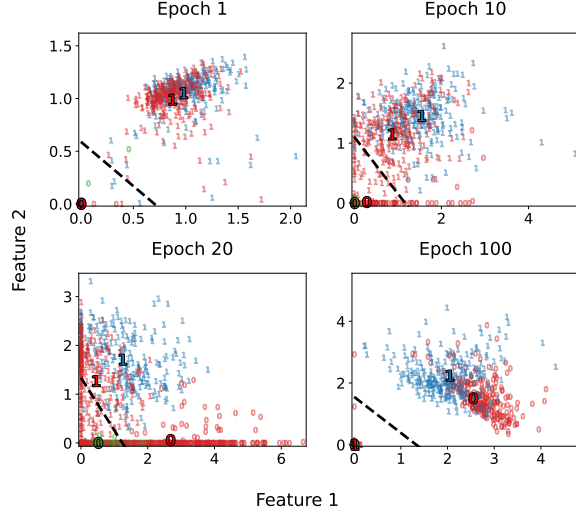


Figure 2: Learned feature representations of the training instances observed at the penultimate layer a MLP comprising an encoder and a classification head at different stages in the training. The data consists of correctly (blue or green resp.) and incorrectly (red) labeled images of zeros and ones from MNIST. The dashed line depicts the linear classifier.

<sup>1</sup>In applications such as image classification, the ground-truth conditional distributions  $p^*(\cdot | \mathbf{x}) \in \mathbb{P}(\mathcal{Y})$  are often degenerate, i.e.,  $p^*(y^* | \mathbf{x}) \approx 1$  and  $p^*(y | \mathbf{x}) \approx 0$  for  $y \neq y^*$ .

towards the other discriminatory face of the decision boundary. This goes hand in hand with a decrease and eventual increase of the predicted probability scores  $\max_{y \in \mathcal{Y}} \hat{p}(y | \mathbf{x})$ , consistent with the observations made in Fig. 1.

It appears natural to seek for means that keep corrupted instances  $(\cdot, y_i)$  close to clean samples  $(\cdot, y_i^*)$  in the feature space, and not let the learning bias in the later stages pull them over towards the label corruption. In the context of the overall optimization, the model itself represents a source for justification whether a class shall be regarded as a plausible outcome or not. Hence, we suggest to use the model predictions *simultaneously* with the training labels as a source for modeling our beliefs about the ground-truth. Consequently, we shall consult not only the individual training labels, but also the *complete* training dataset that found its way into the current model hypothesis in conjunction, complementing the former as a second piece of evidence. This represents a distillation of knowledge obtained from the (mostly clean) data at hand, and we argue that the confidence  $\hat{p}$  is a suitable surrogate to represent plausibility in this regard.

### 3.2 Credal Labeling

Inquiring the model prediction  $\hat{p}(\mathbf{x}_i)$  in addition to the training label  $y_i$  may require to augment the (hitherto single) label by an additional plausible candidate label  $\hat{y}_i \in \operatorname{argmax}_{y' \in \mathcal{Y}} \hat{p}(y' | \mathbf{x}_i)$  with  $\hat{y}_i \neq y_i$ , making the target effectively ambiguous, and hence less convenient for conventional pointwise classification losses. However, from a data modeling perspective, it is important to recognize that the imprecision of the now ambiguous target information pays off with higher validity, i.e., it is more likely that the true label is covered by the target labels. This is completely in line with *data imprecision* in the context of so-called *superset learning* [Lienen and Hüllermeier, 2021a]. Thus, deliberately ambiguating a corrupt training target information appears desirable for dampening the influence of mislabeling.

Before detailing the representation of the aforementioned beliefs, we shall revisit the conventional probabilistic learning setting. To train probabilistic classifiers  $\hat{p}$  as specified above, such as by minimizing the cross-entropy loss, traditional methods transform deterministic target labels  $y_i \in \mathcal{Y}$  as commonly observed in classification datasets into degenerate probability distributions  $p_{y_i} \in \mathbb{P}(\mathcal{Y})$  with  $p_{y_i}(y_i) = 1$  and  $p_{y_i}(y) = 0$  for  $y \neq y_i$ . As a result, the predicted distribution  $\hat{p}$  can be compared to  $p_{y_i}$  using a probabilistic loss  $\mathcal{L} : \mathbb{P}(\mathcal{Y}) \times \mathbb{P}(\mathcal{Y}) \rightarrow \mathbb{R}$  to be optimized in an empirical risk minimization. It is easy to see that full plausibility is assigned to the observed training label  $y_i$ , while the other labels are regarded as fully implausible.

Ambiguity in a probabilistic sense can be attained by enriching the target distribution representation in a set-valued way. To this end, Lienen and Hüllermeier [2021b] propose to use *credal sets*, i.e., sets of probability distributions, as a means to express beliefs about the true class conditional distribution  $p^*$ . Relating to the introductory motivation, we may want to not only consider  $p_{y_i}$  for the training label  $y_i$  as a fully plausible target distribution, but also  $p_y$  for a plausible candidate label  $y \neq y_i$  as well – and interpolations between the two extremes. Credal sets allow one to model such sets of candidate distributions. Moreover, one may also want to consider distributions near the degenerate targets, as it appears unlikely that  $p^*$  is any (extreme) degenerate distribution at all. In other words, one may seek to further *relax* the extremity of the targets by considering neighboring distributions around  $p_{y_i}$  (and possibly  $p_y$ ) as candidate target distributions, relieving from commitment to only degenerate distributions [Lienen and Hüllermeier, 2021b].

To derive credal sets of the described form, possibility theory [Dubois and Prade, 2004] offers a suitable framework by means of so-called *possibility distributions*  $\pi : \mathcal{Y} \rightarrow [0, 1]$ . It induces a possibility measure  $\Pi$  on  $\mathcal{Y}$  by  $\Pi(Y) = \max_{y \in Y} \pi(y)$ . A distribution  $\pi_i$  associated with an instance  $\mathbf{x}_i$  assigns a possibility (or plausibility) to each class in  $\mathcal{Y}$  for being the true class outcome associated with  $\mathbf{x}_i$ . Thus,  $\pi_i(y)$  can be interpreted as an upper probability on  $p^*(y | \mathbf{x}_i)$  inducing a convex credal set:

$$Q_{\pi_i} := \left\{ p \in \mathbb{P}(\mathcal{Y}) \mid \forall Y \subseteq \mathcal{Y} : \sum_{y \in Y} p(y) \leq \max_{y \in Y} \pi_i(y) \right\} \quad (1)$$

### 3.3 Data Ambiguation For Robust Learning

With the theoretical framework to model ambiguous targets in a probabilistic manner, we can put the vision of a robust ambiguation method on a rigorous theoretic foundation. Following the idea of

assigning full plausibility to highly confident class predictions in light of the overall optimization context, we elicit the confidence-thresholded possibility distribution  $\pi_i$  for a training instance  $(\mathbf{x}_i, y_i)$  by

$$\pi_i(y) = \begin{cases} 1 & \text{if } y = y_i \vee \hat{p}(y | \mathbf{x}_i) \geq \beta \\ \alpha & \text{otherwise} \end{cases}, \quad (2)$$

where  $\beta \in [0, 1]$  denotes the confidence threshold for the prediction  $\hat{p}(y | \mathbf{x}_i)$ , and  $\alpha \in [0, 1]$  is the label relaxation parameter [Lienen and Hüllermeier, 2021b]. In fact, the construction of labels by means of Eq. (2) realizes a complementary rather than substitutive pseudo-labeling approach due to retaining full possibility  $\pi_i(y_i) = 1$  for the originally observed training label.

To learn from target sets  $\mathcal{Q}_{\pi_i}$  employing  $\pi_i$ , we make use of generalized risk minimization through the *optimistic superset loss* [Hüllermeier and Cheng, 2015]. This loss is defined as

$$\mathcal{L}^*(\mathcal{Q}_{\pi_i}, \hat{p}) := \min_{p \in \mathcal{Q}_{\pi_i}} \mathcal{L}(p, \hat{p}), \quad (3)$$

which generalizes  $\mathcal{L}$  by a principled data disambiguation of the imprecise targets in light of the entire training data, leading to a minimal empirical risk with respect to  $\mathcal{L}$  in the context of the overall loss minimization.

A common choice for  $\mathcal{L}$  is the Kullback-Leibler divergence  $D_{KL}$ , for which Eq. (3) simplifies to

$$\mathcal{L}^*(\mathcal{Q}_{\pi_i}, \hat{p}) = \begin{cases} 0 & \text{if } \hat{p} \in \mathcal{Q}_{\pi_i} \\ D_{KL}(p^r || \hat{p}) & \text{otherwise} \end{cases}, \quad (4)$$

where

$$p^r(y) = \begin{cases} (1 - \alpha) \cdot \frac{\hat{p}(y)}{\sum_{y' \in \mathcal{Y}: \pi_i(y')=1} \hat{p}(y')} & \text{if } \pi_i(y) = 1 \\ \alpha \cdot \frac{\hat{p}(y)}{\sum_{y' \in \mathcal{Y}: \pi_i(y')=\alpha} \hat{p}(y')} & \text{otherwise} \end{cases}$$

is projecting  $\hat{p}$  onto the boundary of  $\mathcal{Q}_{\pi_i}$ . This loss has proven to be convex and has the same computational complexity as standard losses like cross-entropy Lienen and Hüllermeier [2021b]. In the appendix, we provide a comprehensive algorithmic description of the loss function, confirming the simplicity of our proposal.

Fig. 3 illustrates the core idea of our method, which we will refer to as *Robust Data Ambiguation* (RDA). For a given instance  $(\mathbf{x}, y_1)$ , with  $y_1$  being corrupted from the ground-truth  $y_2$ , we initially observe a probabilistic target centered at  $p_{y_1}$  (and potentially being relaxed by some  $\alpha > 0$ ). Without changing the target, label relaxation would compute the loss by comparing the model prediction  $\hat{p}$  to a (precise) distribution  $p^r$  projecting  $\hat{p}$  towards  $p_{y_1}$ . In this example, the model predicts  $y_2$  with high confidence, thereby exceeding  $\beta$ . With our method, full plausibility would be assigned to  $y_2$  in addition to  $y_1$ , leading to a credal set  $\mathcal{Q}$  as shown in the right plot. To compute the loss,  $\hat{p}$  is now compared to a less extreme target  $p^r$  that is projected onto the larger credal set, not urging the learner to predict distributions close to  $p_{y_1}$ . Consequently, by ambiguating the target set, we relieve the learner from memorizing wrong training labels, but, at the same time, still staying cautious in committing to potentially erroneous model predictions. This de-emphasizes the learning from wrongly labeled training instances, while not affecting the optimization on clean samples in an undesired manner. At the same time, the imprecision allows the model predictions  $\hat{p} \in \mathcal{Q}$  to evolve towards  $p_{y_2}$  driven by the loss minimization of similar instances that are correctly labeled with  $y_2$ .

The parameter  $\beta$  can be seen as a reflector of the trust spent on the model prediction  $\hat{p}$  itself to reason about the plausibility of a class  $y \neq y_i$  being the true outcome  $y^*$ . High values for  $\beta$  indicate that

only highly confident predictions shall adjust the target, whereas less extreme values result in a less cautious model reasoning. Conversely, this also means that classes  $y$  with  $\hat{p}(y) < \beta$  are considered as completely implausible. Hence, small values for  $\beta$  could be also interpreted as exclusion criteria for classes. As shown in a more extensive analysis of the  $\beta$  parameter, the former interpretation is practically more useful in the case of robust classification.

Generally,  $\beta$  could be arbitrarily chosen in  $[0, 1]$ , also adopted to the training progress. As a simple yet effective rule of thumb, we suggest to model  $\beta$  in a decreasing manner: While the model is relatively uncertain in the first epochs, one should not spent to much attention to the model predictions themselves. However, with further progress,  $\hat{p}$  becomes more informative for the confidence-driven possibility elicitation, suggesting to use smaller  $\beta$  values. We found empirically the cosine decaying definition as

$$\beta_T = \beta_1 + \frac{1}{2} (\beta_0 - \beta_1) \left( 1 + \cos \left( \frac{T}{T_{max}} \pi \right) \right), \quad (5)$$

where  $T$  and  $T_{max}$  denote the current and maximum number of epochs, as well as  $\beta_0$  and  $\beta_1$  represent the starting and ending  $\beta$  respectively. Nevertheless, as will be shown in the empirical evaluation, also static values for  $\beta$  work reasonably well, such that the number of additional hyperparameters can be reduced to a single one.

In summary, our robust loss formulation RDA captivates with no adjustment to the training procedure – all computations can be encapsulated in the loss formulation itself with only accessing the model output to derive the possibility distributions –, but providing expressive (on-the-fly) target modeling as offered in (much more complex) label correction methods. This way, it constitutes an easy and, as will be shown in the experiments, effective way to robustify the learning of large models for (probabilistic) classification.

## 4 Experiments

To demonstrate the effectiveness of our method to cope with label noise, we conduct an empirical analysis on a variety of image classification datasets as a practically relevant problem domain. Needless to say, RDA is not specifically tailored to this domain, as it completely refrains from using modality-specific components. Here, we consider CIFAR-10 and -100 [Krizhevsky and Hinton, 2009], as well as the large-scale datasets WebVision [Li et al., 2017] and Clothing1M [Xiao et al., 2015] as benchmark datasets. For the former, we model synthetic noise by both symmetrically and asymmetrically randomizing the labels for a fraction of examples, while WebVision and Clothing1M both comprise real-world noise by their underlying crawling process. Moreover, we report results on CIFAR-10(0)N [Wei et al., 2022b] as another real-world noise datasets based on human annotators. We refer to the appendix for a more detailed description of the datasets and the corruption process, as well as experiments on additional benchmark datasets.

As baselines, we take a wide range of commonly applied loss functions into account. Proceeding from the conventional cross-entropy (CE), we report results for the regularized CE adaptations label smoothing (LS) and label relaxation (LR), as well as the popular robust loss functions generalized cross-entropy (GCE) [Zhang and Sabuncu, 2018], normalized cross-entropy (NCE) [Ma et al., 2020], combinations of NCE with AUL and AGCE [Zhou et al., 2021a] and CORES Cheng et al. [2021]. The mentioned loss functions share that they do not assume any additional model parameters, e.g., to track the trajectories of model predictions. For completeness, we shall also report results violating this assumptions, namely ELR [Liu et al., 2020] and SOP [Liu et al., 2022] as two state-of-the-art representatives for regularization and label correction methods, respectively, albeit constituting an unfair comparison to our off-the-shelf loss. In the appendix, we show further results for a natural baseline to our approach in the realm of superset learning, as well as experiments that combine our method with sample selection.

We follow common practice in evaluating methods against label noise in the regime of overparameterized models by training ResNet34 models on the smaller scale benchmark datasets CIFAR-10/-100. For the larger datasets, we consider ResNet50 models pretrained on ImageNet. All trained models use the same training procedure and optimizer. A more thorough overview over all experimental details, such as hyperparameters and the technical infrastructure, can be found in the appendix. We repeated each run five times with different random seeds, reporting the accuracy on the test splits to measure generalization performance.

Table 1: Test accuracies and standard deviations on the test split for models trained on CIFAR-10(0) with synthetic noise (symmetric or asymmetric). The results are averaged over runs with different seeds, **bold** entries mark the best method without any additional model parameters. Underlined results indicate the best method overall.

Loss	Add. Param.	CIFAR-10				CIFAR-100			
		25 %	Sym. 50 %	75 %	Asym. 40 %	25 %	Sym. 50 %	75 %	Asym. 40 %
CE	<b>X</b>	79.05 $\pm$ 0.67	55.03 $\pm$ 1.02	30.03 $\pm$ 0.74	77.90 $\pm$ 0.31	58.27 $\pm$ 0.36	37.16 $\pm$ 0.46	13.66 $\pm$ 0.45	62.83 $\pm$ 0.25
LS ( $\alpha = 0.1$ )	<b>X</b>	76.66 $\pm$ 0.69	53.95 $\pm$ 1.47	29.03 $\pm$ 1.21	78.07 $\pm$ 0.69	59.75 $\pm$ 0.24	37.61 $\pm$ 0.61	13.53 $\pm$ 0.51	63.76 $\pm$ 0.51
LS ( $\alpha = 0.25$ )	<b>X</b>	77.48 $\pm$ 0.32	53.08 $\pm$ 1.95	28.29 $\pm$ 0.65	77.35 $\pm$ 0.76	59.84 $\pm$ 0.57	39.80 $\pm$ 0.38	14.18 $\pm$ 0.44	63.33 $\pm$ 0.25
LR ( $\alpha = 0.1$ )	<b>X</b>	80.53 $\pm$ 0.39	57.55 $\pm$ 0.95	29.83 $\pm$ 0.87	77.83 $\pm$ 0.37	57.52 $\pm$ 0.58	36.77 $\pm$ 0.54	13.23 $\pm$ 0.14	62.46 $\pm$ 0.15
LR ( $\alpha = 0.25$ )	<b>X</b>	80.43 $\pm$ 0.09	60.18 $\pm$ 1.01	31.36 $\pm$ 0.91	78.35 $\pm$ 0.72	57.67 $\pm$ 0.11	37.15 $\pm$ 0.14	13.41 $\pm$ 0.24	62.85 $\pm$ 0.53
GCE	<b>X</b>	90.82 $\pm$ 0.10	83.36 $\pm$ 0.65	54.34 $\pm$ 0.37	77.37 $\pm$ 0.94	68.06 $\pm$ 0.31	58.66 $\pm$ 0.28	<b>26.85</b> $\pm$ 1.28	61.08 $\pm$ 0.51
NCE	<b>X</b>	79.05 $\pm$ 0.12	63.94 $\pm$ 1.74	38.23 $\pm$ 2.63	76.84 $\pm$ 0.41	19.32 $\pm$ 0.81	11.09 $\pm$ 1.03	6.12 $\pm$ 7.57	24.67 $\pm$ 0.71
NCE+AGCE	<b>X</b>	87.57 $\pm$ 0.10	83.05 $\pm$ 0.81	51.16 $\pm$ 6.44	69.75 $\pm$ 2.33	64.15 $\pm$ 0.23	39.64 $\pm$ 1.66	7.67 $\pm$ 1.25	53.87 $\pm$ 1.60
NCE+AUL	<b>X</b>	88.89 $\pm$ 0.29	84.18 $\pm$ 0.42	<b>65.98</b> $\pm$ 1.56	80.87 $\pm$ 0.34	69.76 $\pm$ 0.31	57.41 $\pm$ 0.41	17.72 $\pm$ 1.27	61.33 $\pm$ 0.55
CORES	<b>X</b>	88.60 $\pm$ 0.28	82.44 $\pm$ 0.29	47.32 $\pm$ 17.03	82.22 $\pm$ 0.55	60.36 $\pm$ 0.67	46.01 $\pm$ 0.44	18.23 $\pm$ 0.28	65.06 $\pm$ 0.41
RDA (ours)	<b>X</b>	<b>91.48</b> $\pm$ 0.22	<b>86.47</b> $\pm$ 0.42	48.11 $\pm$ 15.41	<b>85.95</b> $\pm$ 0.40	<b>70.03</b> $\pm$ 0.32	<b>59.83</b> $\pm$ 1.15	26.75 $\pm$ 8.83	<b>69.62</b> $\pm$ 0.54
ELR	✓	92.45 $\pm$ 0.08	88.39 $\pm$ 0.36	72.58 $\pm$ 1.63	82.18 $\pm$ 0.42	<u>73.66</u> $\pm$ 1.87	48.72 $\pm$ 26.93	38.35 $\pm$ 10.26	74.19 $\pm$ 0.23
SOP	✓	<u>92.58</u> $\pm$ 0.08	<u>89.21</u> $\pm$ 0.33	<u>76.16</u> $\pm$ 4.88	84.61 $\pm$ 0.97	72.04 $\pm$ 0.67	<u>64.28</u> $\pm$ 1.44	<u>40.59</u> $\pm$ 1.62	64.27 $\pm$ 0.34

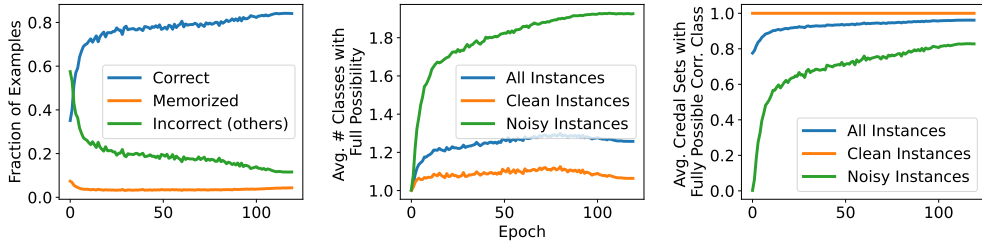


Figure 4: The top plot shows the fraction of mislabeled training instances for which the models predict the ground-truth label (blue), the wrong training label (orange) or a different label (green). The middle and bottom plots show the credal set size and validity respectively. All plots are averaged over the five models trained on CIFAR-10 with 50 % synthetic symmetric noise.

#### 4.1 Synthetic Noise

Table 1 reports the results for the synthetic corruptions on CIFAR-10/-100. As can be seen, our approach provides consistent improvements in terms of generalization performance over the robust off-the-shelf loss functions. Cross-entropy and its regularized adaptations LS and LR appear sensitive to label noise, which confirms the need for robustness on the loss level. Interestingly, although being slightly inferior in most symmetric noise cases, our method proposal appears still competitive compared to ELR and SOP despite their increased expressivity through additional parameters to track the label noise per instance. For asymmetric noise, our method could even outperform such methods. Nevertheless, our method gets less effective with higher amounts of noise.

When looking at the learning dynamics in training with our robust loss proposal, Fig. 4 reveals an effective ambiguation in the course of the learning process. The left plot shows the effective attenuation of any memorization while improving the correctness of model predictions for the wrongly labeled instances at the same time. The plot in the middle depicts an increase of the credal set size in terms of classes with full plausibility for the noisy instances. Together with the right plot showing the validity of the credal sets, i.e., the fraction of credal sets that assign full possibility to the ground-truth class, one can easily see that the ambiguation is indeed able to select the ground-truth class as training label. Furthermore, the credal set size for clean instances is barely affected, supporting the adequacy of our model. Notably, our method also shows self-correcting behavior after ambiguating with a wrong class midway. While the validity of the credal sets increases (roughly) monotonically, the credal set sizes become smaller towards the end of the training, supporting this claim. In the appendix, we provide additional plots in other noise settings showing consistent effects.

Table 2: Test accuracies and standard deviations on the test split for models trained on CIFAR-10(0)N without any noise (clean) and real-world noise. The results are averaged over runs with different seeds, **bold** entries mark the best method without any additional model parameters. Underlined results indicate the best method overall.

Loss	Add. Param.	CIFAR-10N						CIFAR-100N	
		Clean	Random 1	Random 2	Random 3	Aggregate	Worst	Clean	Noisy
CE	✗	<b>94.12</b> $\pm 0.17$	82.96 $\pm 0.23$	83.16 $\pm 0.52$	83.49 $\pm 0.34$	88.74 $\pm 0.13$	64.93 $\pm 0.79$	75.29 $\pm 0.15$	52.88 $\pm 0.14$
LS ( $\alpha = 0.1$ )	✗	93.92 $\pm 0.03$	82.76 $\pm 0.47$	82.10 $\pm 0.21$	82.12 $\pm 0.37$	88.63 $\pm 0.11$	63.10 $\pm 0.38$	75.71 $\pm 0.19$	53.48 $\pm 0.45$
LS ( $\alpha = 0.25$ )	✗	93.71 $\pm 0.40$	82.95 $\pm 1.57$	83.86 $\pm 2.05$	82.61 $\pm 0.25$	87.03 $\pm 2.29$	66.14 $\pm 6.89$	75.69 $\pm 0.17$	53.98 $\pm 0.27$
LR ( $\alpha = 0.1$ )	✗	93.77 $\pm 0.06$	83.00 $\pm 0.36$	82.64 $\pm 0.31$	82.82 $\pm 0.21$	88.41 $\pm 0.29$	66.62 $\pm 0.33$	74.79 $\pm 0.16$	52.01 $\pm 0.04$
LR ( $\alpha = 0.25$ )	✗	93.63 $\pm 0.06$	82.14 $\pm 0.49$	81.87 $\pm 0.34$	82.46 $\pm 0.11$	88.07 $\pm 0.45$	66.44 $\pm 0.14$	74.51 $\pm 0.17$	52.22 $\pm 0.29$
GCE	✗	93.22 $\pm 0.08$	88.85 $\pm 0.19$	88.96 $\pm 0.32$	88.73 $\pm 0.11$	90.85 $\pm 0.32$	77.24 $\pm 0.47$	72.29 $\pm 0.19$	55.43 $\pm 0.47$
NCE	✗	87.67 $\pm 0.25$	81.88 $\pm 0.27$	81.02 $\pm 0.32$	81.48 $\pm 0.13$	84.62 $\pm 0.49$	69.40 $\pm 0.10$	32.31 $\pm 0.31$	21.12 $\pm 0.67$
NCE+AGCE	✗	92.56 $\pm 0.07$	89.48 $\pm 0.28$	88.95 $\pm 0.10$	89.25 $\pm 0.29$	90.65 $\pm 0.44$	81.27 $\pm 0.44$	72.00 $\pm 0.09$	51.42 $\pm 0.65$
NCE+AUL	✗	93.09 $\pm 0.10$	89.42 $\pm 0.22$	89.36 $\pm 0.15$	88.94 $\pm 0.55$	90.92 $\pm 0.19$	81.28 $\pm 0.47$	74.18 $\pm 0.21$	56.58 $\pm 0.41$
CORES	✗	93.09 $\pm 0.08$	86.09 $\pm 0.57$	86.48 $\pm 0.27$	86.02 $\pm 0.22$	89.23 $\pm 0.10$	76.80 $\pm 0.96$	73.70 $\pm 0.17$	53.04 $\pm 0.29$
RDA (ours)	✗	94.09 $\pm 0.19$	<b>90.43</b> $\pm 0.03$	<b>90.09</b> $\pm 0.29$	<b>90.40</b> $\pm 0.01$	<b>91.71</b> $\pm 0.38$	<b>82.91</b> $\pm 0.83$	<b>76.21</b> $\pm 0.64$	<b>59.22</b> $\pm 0.26$
ELR	✓	<u>94.21</u> $\pm 0.11$	<u>91.35</u> $\pm 0.29$	<u>91.46</u> $\pm 0.29$	<u>91.39</u> $\pm 0.03$	<u>92.68</u> $\pm 0.03$	<u>84.82</u> $\pm 0.42$	<u>76.66</u> $\pm 0.11$	<u>62.80</u> $\pm 0.27$
SOP	✓	92.84 $\pm 0.20$	89.16 $\pm 0.40$	89.02 $\pm 0.33$	88.99 $\pm 0.31$	90.54 $\pm 0.16$	80.65 $\pm 0.13$	76.12 $\pm 0.32$	59.32 $\pm 0.41$

Table 3: Large-scale test accuracies on WebVision and Clothing1M using ResNet50 models. The baseline results are for WebVision taken from [Zhou et al., 2021a], whereas the reported accuracies on Clothing1M were taken from [Liu et al., 2020].

Loss	WebVision	Clothing1M
CE	66.96	68.04
GCE	61.76	69.75
AGCE	69.4	-
NCE+AGCE	67.12	-
RDA (ours)	<b>70.23</b>	<b>71.42</b>

## 4.2 Real-World Noise

Consistent to the previous observations, our robust ambiguation loss also work reasonably well for real-world noise. As presented in Table 2, RDA leads to superior generalization performance compared to baselines losses without any additional model parameters in almost any case. Moreover, it also consistently outperforms SOP on CIFAR-10N, whereas it leads to similar results for CIFAR-100N.

For the large-scale datasets WebVision and Clothing1M, whose results are presented in Table 3, one can observe that the differences between the baselines and our approach appear rather subtle, but still in favor of our method proposal.

## 5 Conclusion

Large models are typically prone to memorizing noisy labels in classification tasks. To address this issue, various loss functions have been proposed that enhance the robustness of conventional loss functions against label noise. Although such techniques are appealing due to their simplicity, they typically lack the capacity to incorporate additional knowledge regarding the instances, such as beliefs about the true label. In response, pseudo-labeling methods for label correction have emerged to provide more sophisticated target modeling, albeit at the cost of increased model training complexity.

In our work, we address the shortcomings of previous methods by a simple off-the-shelf loss function that takes the confidence in the model into account to deliberately ambiguate the targets. For labels that appear plausible in light of the overall model training, which we derive from the model’s confidence, this information is used to construct a set-valued target set to represent the beliefs about the true outcome in a complementary, more faithful manner. Our empirical evaluation confirms the adequacy of our proposal.

Our approach poses several interesting future research directions. Among those, a more informed determination of  $\beta$  could be realized by a quantification of epistemic uncertainty [Hüllermeier and Waegeman, 2021] of individual model prediction, as highly uncertain guesses should be considered rather cautiously. Also, our method proposal could also be leveraged for various downstream tasks, e.g., to detect anomalies in mostly homogeneous data. Finally, considering learning trajectories could provide further information to reason about the ground-truth to improve over method, as we are currently only considering the model prediction at a time.

### Acknowledgements

This work was partially supported by the German Research Foundation (DFG) within the Collaborative Research Center “On-The-Fly Computing” (CRC 901 project no. 160364472). Moreover, the authors gratefully acknowledge the funding of this project by computing time provided by the Paderborn Center for Parallel Computing (PC<sup>2</sup>).

### References

E. Arazo, D. Ortego, P. Albert, N. E. O’Connor, and K. McGuinness. Unsupervised label noise modeling and loss correction. In *Proc. of the 36th International Conference on Machine Learning, ICML, June 9-15, Long Beach, California, USA*, volume 97 of *Proc. of Machine Learning Research*, pages 312–321. PMLR, 2019.

D. Arpit, S. Jastrzebski, N. Ballas, D. Krueger, E. Bengio, M. S. Kanwal, T. Maharaj, A. Fischer, A. C. Courville, Y. Bengio, and S. Lacoste-Julien. A closer look at memorization in deep networks. In *Proc. of the 34th International Conference on Machine Learning, ICML, August 6-11, Sydney, NSW, Australia*, volume 70 of *Proc. of Machine Learning Research*, pages 233–242. PMLR, 2017.

P. Bachman, O. Alsharif, and D. Precup. Learning with pseudo-ensembles. In *Advances in Neural Information Processing Systems 27: Annual Conference on Neural Information Processing Systems, NIPS, December 8-13, Montreal, Quebec, Canada*, pages 3365–3373, 2014.

H. Chang, E. G. Learned-Miller, and A. McCallum. Active bias: Training more accurate neural networks by emphasizing high variance samples. In *Advances in Neural Information Processing Systems 30: Annual Conference on Neural Information Processing Systems, December 4-9, Long Beach, CA, USA*, pages 1002–1012, 2017.

W. Chen, C. Zhu, and Y. Chen. Sample prior guided robust model learning to suppress noisy labels. *CoRR*, abs/2112.01197, 2021.

H. Cheng, Z. Zhu, X. Li, Y. Gong, X. Sun, and Y. Liu. Learning with instance-dependent label noise: A sample sieve approach. In *9th International Conference on Learning Representations, ICLR, May 3-7, Virtual Event, Austria*. OpenReview.net, 2021.

D. Dubois and H. Prade. Possibility theory, probability theory and multiple-valued logics: A clarification. *Annals of Mathematics and Artificial Intelligence*, 32:35–66, 2004.

L. Feng, S. Shu, Z. Lin, F. Lv, L. Li, and B. An. Can cross entropy loss be robust to label noise? In *Proc. of the Twenty-Ninth International Joint Conference on Artificial Intelligence, IJCAI*, pages 2206–2212. ijcai.org, 2020.

A. Ghosh, H. Kumar, and P. S. Sastry. Robust loss functions under label noise for deep neural networks. In *Proc. of the 31st AAAI Conference on Artificial Intelligence, February 4-9, San Francisco, California, USA*, pages 1919–1925. AAAI Press, 2017.

J. Goldberger and E. Ben-Reuven. Training deep neural-networks using a noise adaptation layer. In *5th International Conference on Learning Representations, ICLR, April 24-26, Toulon, France, Conference Track Proc*. OpenReview.net, 2017.

X. Gui, W. Wang, and Z. Tian. Towards understanding deep learning from noisy labels with small-loss criterion. In *Proc. of the Thirtieth International Joint Conference on Artificial Intelligence, IJCAI, August 19-27, Virtual Event / Montreal, Canada*, pages 2469–2475. ijcai.org, 2021.

B. Han, Q. Yao, X. Yu, G. Niu, M. Xu, W. Hu, I. W. Tsang, and M. Sugiyama. Co-teaching: Robust training of deep neural networks with extremely noisy labels. In *Advances in Neural Information Processing Systems 31: Annual Conference on Neural Information Processing Systems, NeurIPS, December 3-8, Montréal, Canada*, pages 8536–8546, 2018.

E. Hüllermeier and W. Cheng. Superset learning based on generalized loss minimization. In *Proc. of the European Conference on Machine Learning and Knowledge Discovery in Databases, ECML PKDD, September 7-11, Porto, Portugal, Proc. Part II*, volume 9285 of *LNCS*, pages 260–275. Springer, 2015.

E. Hüllermeier and W. Waegeman. Aleatoric and epistemic uncertainty in machine learning: an introduction to concepts and methods. *Mach. Learn.*, 110(3):457–506, 2021.

A. Iscen, J. Valmadre, A. Arnab, and C. Schmid. Learning with neighbor consistency for noisy labels. In *IEEE/CVF Conference on Computer Vision and Pattern Recognition, CVPR, June 18-24, New Orleans, LA, USA*, pages 4662–4671. IEEE, 2022.

L. Jiang, Z. Zhou, T. Leung, L. Li, and L. Fei-Fei. MentorNet: Learning data-driven curriculum for very deep neural networks on corrupted labels. In *Proc. of the 35th International Conference on Machine Learning, ICML, July 10-15, Stockholm, Sweden*, volume 80 of *Proc. of Machine Learning Research*, pages 2309–2318. PMLR, 2018.

A. Krizhevsky and G. Hinton. Learning multiple layers of features from tiny images. Technical report, University of Toronto, Toronto, Canada, 2009.

S. M. Kye, K. Choi, J. Yi, and B. Chang. Learning with noisy labels by efficient transition matrix estimation to combat label miscorrection. In *17th European Conference on Computer Vision ECCV, Tel Aviv, October 23-27, Israel, Proc. Part XXV*, volume 13685 of *Lecture Notes in Computer Science*, pages 717–738. Springer, 2022.

Y. LeCun, L. Bottou, Y. Bengio, and P. Haffner. Gradient-based learning applied to document recognition. *Proc. of the IEEE*, 86(11):2278–2324, 1998.

J. Li, R. Socher, and S. C. H. Hoi. DivideMix: Learning with noisy labels as semi-supervised learning. In *8th International Conference on Learning Representations, ICLR, April 26-30, Addis Ababa, Ethiopia*. OpenReview.net, 2020.

W. Li, L. Wang, W. Li, E. Agustsson, and L. V. Gool. WebVision database: Visual learning and understanding from web data. *CoRR*, abs/1708.02862, 2017.

J. Lienen and E. Hüllermeier. Instance weighting through data imprecision. *Int. J. Approx. Reason.*, 134:1–14, 2021a.

J. Lienen and E. Hüllermeier. From label smoothing to label relaxation. In *Proc. of the 35th AAAI Conference on Artificial Intelligence, February 2-9, Virtual Event*, pages 8583–8591. AAAI Press, 2021b.

L. Liu and T. Dietterich. Learnability of the superset label learning problem. In *Proc. ICML 2014, Int. Conf. on Machine Learning*, Beijing, China, 2014.

S. Liu, J. Niles-Weed, N. Razavian, and C. Fernandez-Granda. Early-learning regularization prevents memorization of noisy labels. In *Advances in Neural Information Processing Systems 33: Annual Conference on Neural Information Processing Systems, NeurIPS, December 6-12, Virtual Event*, 2020.

S. Liu, Z. Zhu, Q. Qu, and C. You. Robust training under label noise by over-parameterization. In *Proc. of the 39th International Conference on Machine Learning, ICML, July 17-23, Baltimore, Maryland, USA*, volume 162 of *Proc. of Machine Learning Research*, pages 14153–14172. PMLR, 17–23 Jul 2022.

Y. Lu and W. He. SELC: self-ensemble label correction improves learning with noisy labels. In L. D. Raedt, editor, *Proc. of the Thirty-First International Joint Conference on Artificial Intelligence, IJCAI, July 23-29, Vienna, Austria*, pages 3278–3284. ijcai.org, 2022.

M. Lukasik, S. Bhojanapalli, A. K. Menon, and S. Kumar. Does label smoothing mitigate label noise? *ArXiv*, abs/2003.02819, 2020.

J. Ma and S. Fattah. Blessing of nonconvexity in deep linear models: Depth flattens the optimization landscape around the true solution. *CoRR*, abs/2207.07612, 2022.

X. Ma, H. Huang, Y. Wang, S. Romano, S. M. Erfani, and J. Bailey. Normalized loss functions for deep learning with noisy labels. In *Proc. of the 37th International Conference on Machine Learning, ICML, July 13-18, Virtual Event*, volume 119 of *Proc. of Machine Learning Research*, pages 6543–6553. PMLR, 2020.

A. K. Menon, A. S. Rawat, S. J. Reddi, and S. Kumar. Can gradient clipping mitigate label noise? In *8th International Conference on Learning Representations, ICLR, April 26-30, Addis Ababa, Ethiopia*. OpenReview.net, 2020.

Y. Netzer, T. Wang, A. Coates, A. Bissacco, B. Wu, and A. Y. Ng. Reading digits in natural images with unsupervised feature learning. In *Advances in Neural Information Processing Systems 33: Annual Conference on Neural Information Processing Systems, NIPS, November 12-17, Granada, Spain, Workshop on Deep Learning and Unsupervised Feature Learning*, 2011.

D. A. Nguyen, R. Levie, J. Lienen, G. Kutyniok, and E. Hüllermeier. Memorization-dilation: Modeling neural collapse under noise. *CoRR*, abs/2206.05530, 2022.

K. Nishi, Y. Ding, A. Rich, and T. Höllerer. Augmentation strategies for learning with noisy labels. In *IEEE Conference on Computer Vision and Pattern Recognition, CVPR, June 19-25, Virtual Event*, pages 8022–8031. Computer Vision Foundation / IEEE, 2021.

V. Petyan, X. Y. Han, and D. L. Donoho. Prevalence of neural collapse during the terminal phase of deep learning training. *Proc. of the National Academy of Sciences of the United States of America*, 117:24652 – 24663, 2020.

G. Patrini, A. Rozza, A. K. Menon, R. Nock, and L. Qu. Making deep neural networks robust to label noise: A loss correction approach. In *IEEE Conference on Computer Vision and Pattern Recognition, CVPR, July 21-26, Honolulu, HI, USA*, pages 2233–2241. IEEE Computer Society, 2017.

S. E. Reed, H. Lee, D. Anguelov, C. Szegedy, D. Erhan, and A. Rabinovich. Training deep neural networks on noisy labels with bootstrapping. In *3rd International Conference on Learning Representations, ICLR, May 7-9, San Diego, CA, USA, Workshop Track Proc.*, 2015.

Y. Shen and S. Sanghavi. Learning with bad training data via iterative trimmed loss minimization. In *Proc. of the 36th International Conference on Machine Learning, ICML, June 9-15, Long Beach, California, USA*, volume 97 of *Proc. of Machine Learning Research*, pages 5739–5748. PMLR, 2019.

K. Sohn, D. Berthelot, N. Carlini, Z. Zhang, H. Zhang, C. Raffel, E. D. Cubuk, A. Kurakin, and C. Li. FixMatch: Simplifying semi-supervised learning with consistency and confidence. In *Advances in Neural Information Processing Systems 33: Annual Conference on Neural Information Processing Systems, NeurIPS, December 6-12, Virtual Event*, 2020.

H. Song, M. Kim, and J. Lee. SELFIE: refurbishing unclean samples for robust deep learning. In *Proc. of the 36th International Conference on Machine Learning, ICML, June 9-15, Long Beach, California, USA*, volume 97 of *Proc. of Machine Learning Research*, pages 5907–5915. PMLR, 2019.

H. Song, M. Kim, D. Park, and J. Lee. Learning from noisy labels with deep neural networks: A survey. *CoRR*, abs/2007.08199, 2020.

N. Srivastava, G. E. Hinton, A. Krizhevsky, I. Sutskever, and R. Salakhutdinov. Dropout: a simple way to prevent neural networks from overfitting. *J. Mach. Learn. Res.*, 15(1):1929–1958, 2014.

C. Szegedy, V. Vanhoucke, S. Ioffe, J. Shlens, and Z. Wojna. Rethinking the inception architecture for computer vision. In *Proc. of the IEEE Conference on Computer Vision and Pattern Recognition, CVPR, June 27-30, Las Vegas, NV, USA*, pages 2818–2826. IEEE Computer Society, 2016.

D. Tanaka, D. Ikami, T. Yamasaki, and K. Aizawa. Joint optimization framework for learning with noisy labels. In *IEEE Conference on Computer Vision and Pattern Recognition, CVPR, June 18-22, Salt Lake City, UT, USA*, pages 5552–5560. Computer Vision Foundation / IEEE Computer Society, 2018.

M. Toneva, A. Sordoni, R. T. des Combes, A. Trischler, Y. Bengio, and G. J. Gordon. An empirical study of example forgetting during deep neural network learning. In *7th International Conference on Learning Representations, ICLR, May 6-9, New Orleans, LA, USA*. OpenReview.net, 2019.

Y. Tu, B. Zhang, Y. Li, L. Liu, J. Li, Y. Wang, C. Wang, and C. Zhao. Learning from noisy labels with decoupled meta label purifier. *CoRR*, abs/2302.06810, 2023.

H. Wang, R. Xiao, Y. Dong, L. Feng, and J. Zhao. ProMix: Combating label noise via maximizing clean sample utility. *CoRR*, abs/2207.10276, 2022.

Y. Wang, X. Ma, Z. Chen, Y. Luo, J. Yi, and J. Bailey. Symmetric cross entropy for robust learning with noisy labels. In *IEEE/CVF International Conference on Computer Vision, ICCV, October 27 - November 2, Seoul, Korea (South)*, pages 322–330. IEEE, 2019.

H. Wei, L. Feng, X. Chen, and B. An. Combating noisy labels by agreement: A joint training method with co-regularization. In *IEEE/CVF Conference on Computer Vision and Pattern Recognition, CVPR, June 13-19, Seattle, WA, USA*, pages 13723–13732. Computer Vision Foundation / IEEE, 2020.

J. Wei and Y. Liu. When optimizing f-divergence is robust with label noise. In *9th International Conference on Learning Representations, ICLR, May 3-7, Virtual Event*. OpenReview.net, 2021.

J. Wei, H. Liu, T. Liu, G. Niu, M. Sugiyama, and Y. Liu. To smooth or not? when label smoothing meets noisy labels. In *Proc. of the 39th International Conference on Machine Learning, ICML, July 17-23, Baltimore, Maryland, USA*, volume 162 of *Proc. of Machine Learning Research*, pages 23589–23614. PMLR, 2022a.

J. Wei, Z. Zhu, H. Cheng, T. Liu, G. Niu, and Y. Liu. Learning with noisy labels revisited: A study using real-world human annotations. In *10th International Conference on Learning Representations, ICLR, April 25-29, Virtual Event*. OpenReview.net, 2022b.

Y. Wu, J. Shu, Q. Xie, Q. Zhao, and D. Meng. Learning to purify noisy labels via meta soft label corrector. In *Proc. of the Thirty-Fifth AAAI Conference on Artificial Intelligence, AAAI, February 2-9, Virtual Event*, pages 10388–10396. AAAI Press, 2021.

H. Xiao, K. Rasul, and R. Vollgraf. Fashion-MNIST: A novel image dataset for benchmarking machine learning algorithms. *CoRR*, abs/1708.07747, 2017.

T. Xiao, T. Xia, Y. Yang, C. Huang, and X. Wang. Learning from massive noisy labeled data for image classification. In *IEEE Conference on Computer Vision and Pattern Recognition, CVPR, June 7-12, Boston, MA, USA*, pages 2691–2699. IEEE Computer Society, 2015.

Y. Yao, Z. Sun, C. Zhang, F. Shen, Q. Wu, J. Zhang, and Z. Tang. Jo-SRC: A contrastive approach for combating noisy labels. In *IEEE Conference on Computer Vision and Pattern Recognition, CVPR, June 19-25, Virtual Event*, pages 5192–5201. Computer Vision Foundation / IEEE, 2021.

X. Yu, B. Han, J. Yao, G. Niu, I. W. Tsang, and M. Sugiyama. How does disagreement help generalization against label corruption? In *Proc. of the 36th International Conference on Machine Learning, ICML, June 9-15, Long Beach, California, USA*, volume 97 of *Proc. of Machine Learning Research*, pages 7164–7173. PMLR, 2019.

Y. Yu, K. H. R. Chan, C. You, C. Song, and Y. Ma. Learning diverse and discriminative representations via the principle of maximal coding rate reduction. In *Advances in Neural Information Processing Systems 33: Annual Conference on Neural Information Processing Systems, NeurIPS, December 6-12, Virtual Event*, 2020.

Z. Zhang and M. R. Sabuncu. Generalized cross entropy loss for training deep neural networks with noisy labels. In *Advances in Neural Information Processing Systems 31: Annual Conference on Neural Information Processing Systems, NeurIPS, December 3-8, Montréal, Canada*, pages 8792–8802, 2018.

E. Zheltonozhskii, C. Baskin, A. Mendelson, A. M. Bronstein, and O. Litany. Contrast to divide: Self-supervised pre-training for learning with noisy labels. In *IEEE/CVF Winter Conference on Applications of Computer Vision, WACV, January 3-8, Waikoloa, HI, USA*, pages 387–397. IEEE, 2022.

X. Zhou, X. Liu, J. Jiang, X. Gao, and X. Ji. Asymmetric loss functions for learning with noisy labels. In *Proc. of the 38th International Conference on Machine Learning, ICML, July 18-24, Virtual Event*, volume 139 of *Proc. of Machine Learning Research*, pages 12846–12856. PMLR, 2021a.

X. Zhou, X. Liu, C. Wang, D. Zhai, J. Jiang, and X. Ji. Learning with noisy labels via sparse regularization. In *IEEE/CVF International Conference on Computer Vision, ICCV, October 10-17, Montreal, QC, Canada*, pages 72–81. IEEE, 2021b.

Z. Zhu, J. Wang, and Y. Liu. Beyond images: Label noise transition matrix estimation for tasks with lower-quality features. In *Proc. of the 39th International Conference on Machine Learning, ICML, July 17-23, Baltimore, Maryland, USA*, volume 162 of *Proc. of Machine Learning Research*, pages 27633–27653. PMLR, 2022.

## A Algorithmic RDA Loss Description

Algorithm 1 provides a pseudo-code description of the loss calculation per batch in the RDA approach.

---

### Algorithm 1 Robust Data Ambiguation (RDA) Loss Calculation

---

**Require:** Training instance  $(\mathbf{x}, y) \in \mathcal{X} \times \mathcal{Y}$ , model prediction  $\hat{p}(\mathbf{x}) \in \mathbb{P}(\mathcal{Y})$ , confidence threshold  $\beta \in [0, 1]$ , relaxation parameter  $\alpha \in [0, 1]$

1: Construct  $\pi$  as in Eq. (4) with

$$\pi(y') = \begin{cases} 1 & \text{if } y' = y \vee \hat{p}(y' | \mathbf{x}) \geq \beta \\ \alpha & \text{otherwise} \end{cases}$$

2: **return**  $\mathcal{L}^*(Q_\pi, \hat{p}(\mathbf{x}))$  as specified in Eq. (4), where  $Q_\pi$  is derived from  $\pi$

---

## B Evaluation Details

### B.1 Dataset and Data Preprocessing

As datasets, we consider a wide range of commonly studied image classification datasets. While CIFAR-10 and -100 [Krizhevsky and Hinton, 2009], MNIST [LeCun et al., 1998], FashionMNIST [Xiao et al., 2017] and SVHN [Netzer et al., 2011] (the latter three are used in an additional study in Sec. C.3) are widely known and well-studied, WebVision [Li et al., 2017] and Clothing1M [Xiao et al., 2015] comprise real-world noise from human annotations. For WebVision (version 1.0), we consider the Google image subset of ca. 66,000 images from the top-50 classes resized to 256x256. Clothing1M consists of 1 million training images with noisy and 10,000 test images with clean labels. Here, we also resize the images to 256x256.

For training, we apply data augmentation to the training images as commonly being done in image classification. To do so, we randomly crop images of size 32 (CIFAR-10(0)(N), SVHN), 227 (WebVision) or 224 (Clothing1M), followed by horizontally flipping the image with probability of 0.5. In case of MNIST and FashionMNIST, we keep the images unchanged, but resize them to size 32. The reported dimensions are used to preserve comparability with previous results (e.g., as reported in [Liu et al., 2020]).

### B.2 Synthetic Noise Model

While CIFAR-10N and -100N [Wei et al., 2022b], WebVision and Clothing1M provide real-world noise in the standard annotations, we modeled additional label corruptions for the rest of the datasets in a synthetic manner. Thereby, we distinguish symmetric and asymmetric noise: For the former, each class is treated equally, whereas the asymmetric noise applies individual corruptions to each class.

In case of the symmetric noise, we flip a parameterized fraction  $\rho \in [0, 1]$  of instances by uniformly sampling the label from all classes, i.e., we sample a corrupted label via  $y \sim \text{Unif}(\mathcal{Y})$  from the uniform distribution  $\text{Unif}(\mathcal{Y})$  over the class space  $\mathcal{Y}$  with probability  $\rho$ . Hence, also correct label can be chosen again. In our studies, we considered values  $\rho \in \{0.25, 0.5, 0.75\}$ .

In case of asymmetric noise, we use the same setup as suggested in [Patrini et al., 2017]. For CIFAR-10, we flip “truck” to “automobile”, “bird” to “airplane”, “deer” to “horse”, as well as interchange “cat” and “dog”. For CIFAR-100, the classes are grouped into 20 clusters with 5 classes each, whereby labels are flipped within these clusters in a round-robin fashion. In both cases, we apply asymmetric random flips with probability  $\rho = 0.4$ .

### B.3 Hyperparameters

In our paper, we follow common evaluation settings as in recent label noise robustness approaches [Zhou et al., 2021a, Liu et al., 2022]. To this end, we keep the optimizer hyperparameters as being used in previous reports, allowing for a fair comparison. Table 4 gives an overview over used hyperparameters. In all case, we used SGD with momentum of 0.9 as optimizer.

Table 4: Hyperparameters fixed for all baselines and our method per dataset. ResNet50 models proceed from model weights pretrained on ImageNet.

	CIFAR-10(N)	CIFAR-100(N)	WebVision	Clothing1M
Model	ResNet34	ResNet34	ResNet50 (pretrained)	ResNet50 (pretrained)
Batch size	128	128	64	32
Learning rate (LR)	0.02	0.02	0.02	0.002
LR decay	cosine	cosine	cosine	cosine
Weight decay	$5 \times 10^{-4}$	$5 \times 10^{-4}$	$5 \times 10^{-4}$	$1 \times 10^{-3}$
Epochs	120	150	100	15

For the individual losses, we used the optimal parameters being reported in the respective works. This is reasonable as these parameters were optimized in a similar manner on the same data, such that we can re-use these optimization results. For our losses, we fixed the parameters as specified above and optimized the  $\beta$  parameters using random search with 20 iterations employing a 5-fold cross validation on the (partially noisy) training data. To ensure this optimization does not give our method an unfair advantage, we performed the same operation to samples of the baseline experiments, where we noticed that the optimization preferred similar hyperparameter combinations as also reported in the related work.

For results presented in the main paper, we used a cosine decaying strategy as shown in Eq. (5) with  $\beta_0 = 0.75$  and  $\beta_1 = 0.6$  on all datasets except CIFAR-100. On the latter, we used a fixed schedule with  $\beta = 0.5$ . In Section C.2, we further present an ablation study showing results for different  $\beta$  schedules. In all cases, we set  $\alpha = 0.05$ .

#### B.4 Technical Infrastructure

The code of our empirical evaluation is made publicly available<sup>2</sup>. All experiments are implemented using PyTorch<sup>3</sup> as deep learning framework using Nvidia CUDA<sup>4</sup> as acceleration backend. Image manipulations as being used for data agumentation are provided by Pillow<sup>5</sup>. To perform the experiments, we used several Nvidia A100 and RTX 2080 Ti accelerators in a modern high performance computing environment.

### C Further Experiments

#### C.1 Comparison to Full Ambiguation

In this section, we compare our method RDA to a full ambiguation adaptation: For prediction  $\hat{p}$  exceeding  $\beta$  for a class different to the training label, we ambiguate the target information by a completely agnostic credal sets. Hence, this instance is completely ignored in the loss optimization. Table 5 shows the respective results, where significant improvements over the complete ambiguation can be observed for our method. Hence, incorporating credal sets with two fully plausible classes appears reasonable from a loss minimization context.

#### C.2 Parameter Ablation

##### C.2.1 Schedules

In our paper, we proposed to use a cosine decaying strategy to determine  $\beta$ , reflecting an increase in the certainty of the model over the course of the training. Here, we compare this strategy to two alternative schedules, namely a constant and a linear function. Table 6 shows the respective results, where the more sophisticated schedules appear to be superior compared to the constant function.

<sup>2</sup>See <https://github.com/julilien/MitigatingLabelNoiseDataAmbiguation> for our official implementation.

<sup>3</sup><https://pytorch.org/>, BSD-3 license

<sup>4</sup><https://developer.nvidia.com/cuda-toolkit>

<sup>5</sup><https://python-pillow.org/>, HPND License

Table 5: Averaged test accuracies and standard deviations computed over three runs with different seeds. **Bold** entries mark the best method.

	CIFAR-10N	RDA	Complete Ambig.
Clean	<b>94.09</b> $\pm 0.19$	93.77 $\pm 0.37$	
Random1	<b>90.43</b> $\pm 0.03$	87.04 $\pm 0.18$	
Random2	<b>90.09</b> $\pm 0.29$	89.36 $\pm 0.16$	
Random3	<b>90.40</b> $\pm 0.01$	89.04 $\pm 0.21$	
Aggregate	<b>91.71</b> $\pm 0.38$	88.73 $\pm 0.64$	
Worst	<b>82.91</b> $\pm 0.83$	76.57 $\pm 0.91$	

Table 6: Averaged test accuracies and standard deviations computed over three runs with different seeds. **Bold** entries mark the best method.

Schedule	CIFAR-10		
	25 %	50 %	75 %
Constant ( $\beta = 0.75$ )	90.72 $\pm 0.44$	83.97 $\pm 0.81$	54.33 $\pm 11.70$
Linear ( $\beta_0 = 0.75, \beta_1 = 0.6$ )	91.35 $\pm 0.29$	85.16 $\pm 1.48$	35.50 $\pm 1.52$
Cosine ( $\beta_0 = 0.75, \beta_1 = 0.6$ )	<b>91.41</b> $\pm 0.27$	<b>86.46</b> $\pm 0.47$	<b>56.83</b> $\pm 1.71$

### C.2.2 Varying $\beta_0$ and $\beta_1$

Table 7: Results for different  $\beta_1$  parameters with  $\beta_0 = 0.75$  using a cosine decaying  $\beta$  schedule. **Bold** entries mark the best parameter.

$\beta_1$	CIFAR-10	
	25 %	50 %
0.75	90.93	83.74
0.6	91.32	84.21
0.5	<b>91.65</b>	<b>85.98</b>
0.4	85.72	66.11
0.3	81.89	41.93
0.2	78.49	11.79

Table 8: Results for different  $\beta_0$  parameters with  $\beta_1 = 0.5$  using a cosine decaying  $\beta$  schedule. **Bold** entries mark the best parameter.

$\beta_0$	CIFAR-10	
	25 %	50 %
0.8	<b>90.18</b>	<b>82.63</b>
0.75	89.41	81.71
0.7	88.17	80.58
0.6	86.14	78.44
0.5	69.20	65.71

In another study, we look how changes in  $\beta_0$  and  $\beta_1$  for the cosine schedule behave in terms of generalization performance. The respective results are shown in Table 7 and 8.

### C.3 Simplified Setting

Relating to the phenomenon of neural collapse [Papyan et al., 2020], we study the effects of our method in a simplified setting. More precisely, we consider multi-layer perceptron models consisting of a feature encoder and a classification head. The models consist of 6 dense layers with a width of 2048 neurons. To conform with previous studies [Nguyen et al., 2022], we restrict the number of features at the last encoder layer to the number of classes  $K$  in the datasets. We consider the datasets

MNIST, FashionMNIST and SVHN, from which we sample classes  $K \in \{2, 3, 5, 10\}$ . Apart from the model, we use the same hyperparameters as described in Table 4 for CIFAR-10. We used the same setup to construct Figure 3 as shown in the main paper. For  $K = 2$ , we can readily investigate the learned feature representations over the course of the training in a convenient manner.

These experiments aim to provide further evidence for the generalization of our method in more restricted settings under simplified model assumptions. Table 9 shows the results, where a consistent improvement of our method compared to typically considered neural collapsing functions can be observed. This suggests that our method is also applicable for more restricted models than typically considered overparameterized models.

Table 9: Test accuracies on the three additional benchmark datasets using a simplified MLP with a restricted feature space at the penultimate layer. **Bold** entries mark the best method.

Loss	MNIST				FashionMNIST				SVHN			
	$K = 2$	$K = 3$	$K = 5$	$K = 10$	$K = 2$	$K = 3$	$K = 5$	$K = 10$	$K = 2$	$K = 3$	$K = 5$	$K = 10$
CE	73.19	67.59	68.44	66.24	78.60	68.33	65.68	59.51	76.60	65.65	58.59	50.57
LS ( $\alpha = 0.1$ )	74.04	66.44	72.19	71.24	81.45	72.23	67.60	62.78	79.66	68.97	61.74	52.72
LR ( $\alpha = 0.1$ )	73.66	66.00	66.34	64.58	80.15	69.43	64.20	57.25	76.63	67.00	58.62	49.98
RDA (ours)	<b>97.59</b>	<b>90.78</b>	<b>87.86</b>	<b>82.75</b>	<b>92.45</b>	<b>91.63</b>	<b>82.36</b>	<b>77.13</b>	<b>86.77</b>	<b>73.03</b>	<b>65.67</b>	<b>53.98</b>

#### C.4 Combination with Sample Selection

In additional experiments, we integrated our RDA approach in a sample selection approach based on the small loss criterion [Gui et al., 2021], as also been applied in more sophisticated (semi-supervised) approaches that add substantial complexity to the learning setup. To this end, we train the model for 3 epochs on CIFAR-10(N)-100 with cross-entropy based on the training examples, and take the 10 % training instances with the smallest cross-entropy loss. For these instances, we fix the label, i.e., we do not allow any ambiguity such that these instances serve as a corrective. Then, we train the model with our RDA loss as described in Algorithm 1 with the hyperparameters reported in Tab. 4. In the following, we will refer to this variant as *RDA\**.

Table 10: Test accuracies and standard deviations on the test split for models trained on CIFAR-10(0) with synthetic noise. The results are averaged over runs with different seeds, **bold** entries mark the best performing method per column.

Method	CIFAR-10			CIFAR-100		
	25 %	50 %	75 %	25 %	50 %	75 %
RDA	$91.48 \pm 0.22$	$86.47 \pm 0.42$	$48.11 \pm 15.41$	<b>70.03</b> $\pm 0.32$	$59.83 \pm 1.15$	$26.75 \pm 8.83$
RDA*	<b>91.79</b> $\pm 0.21$	<b>86.78</b> $\pm 0.50$	<b>67.08</b> $\pm 2.09$	$69.98 \pm 0.17$	<b>60.18</b> $\pm 1.18$	<b>30.82</b> $\pm 9.45$

Table 11: Test accuracies and standard deviations on the test split for models trained on CIFAR-10N with synthetic noise. The results are averaged over runs with different seeds, **bold** entries mark the best performing method per column.

Method	CIFAR-10N					
	Clean	Random 1	Random 2	Random 3	Aggregate	Worst
RDA	$94.09 \pm 0.19$	$90.43 \pm 0.03$	$90.09 \pm 0.29$	$90.40 \pm 0.01$	$91.71 \pm 0.38$	$82.91 \pm 0.83$
RDA*	<b>94.15</b> $\pm 0.05$	<b>90.76</b> $\pm 0.13$	<b>90.55</b> $\pm 0.37$	<b>90.86</b> $\pm 0.09$	<b>91.84</b> $\pm 0.18$	<b>83.79</b> $\pm 0.24$

As can be seen in the results present in Tables 10 and 11, RDA\* can achieve almost consistently better performance with this addition, confirming its flexibility in being employed in more sophisticated setups. Notably, RDA\* shows the largest improvement in robustness in the high noise regime (75 % noise).

## D Additional Training Behavior Plots

### D.1 CIFAR-10

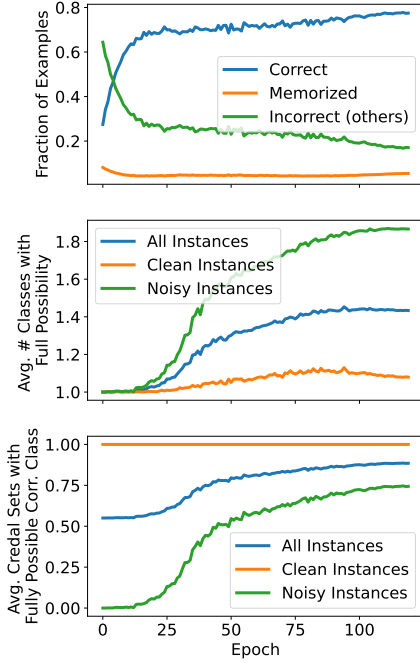


Figure 5: The training behavior of our method on CIFAR-10 with 50 % label noise averaged over five different seeds.

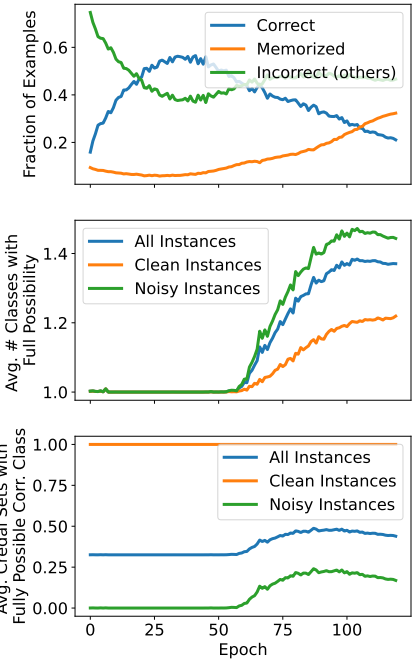


Figure 6: The training behavior of our method on CIFAR-10 with 75 % label noise averaged over five different seeds.

## D.2 CIFAR-100

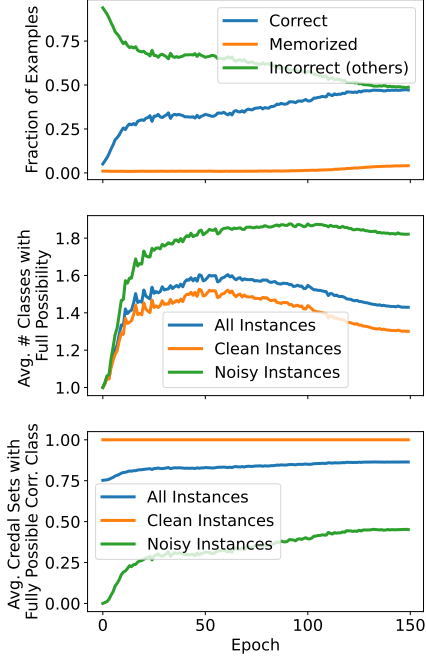


Figure 7: The training behavior of our method on CIFAR-100 with 25 % label noise averaged over five different seeds.

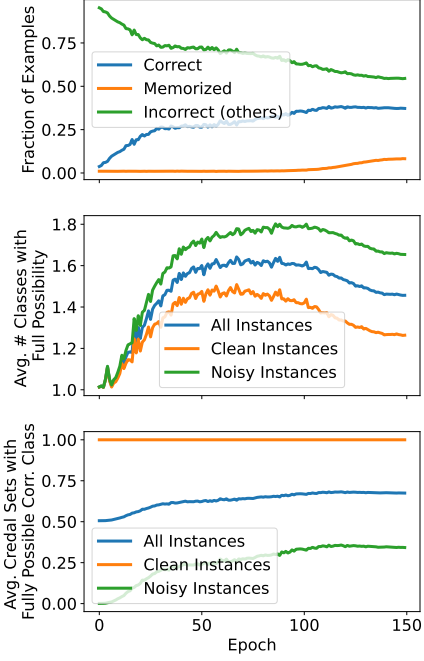


Figure 8: The training behavior of our method on CIFAR-100 with 50 % label noise averaged over five different seeds.

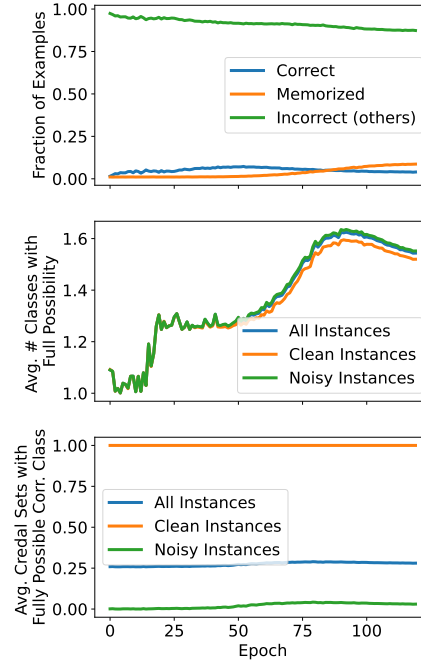


Figure 9: The training behavior of our method on CIFAR-100 with 75 % label noise averaged over five different seeds.